MEMS-driven Flexible Filters for Cognitive Radio

Bruce E. Carey-Smith, Paul A. Warr & Mark A. Beach

Abstract—**This paper describes a discretely tunable filter topology based on lumped-distributed coupled transmission-lines, particularly suitable for micro-electro-mechanical systems switching devices. This topology is capable of simultaneous wide-band centre-frequency and bandwidth tuning. Low fractional bandwidths can be achieved without the need for large coupled-line spacings due to the anti-phase relationship of the lumped capacitive and distributed electro-magnetic coupling coefficients. Both simulated and measured results are presented and discussed.**

I. INTRODUCTION

INVESTIGATION into the implementation of cognitive radio has highlighted the importance of flexible receiver front-end filtering [1]. A single reconfigurable filter capable of operating over the complete range is likely to offer significant savings in terms of size and system complexity.

The continuing maturation of radio frequency micro-electro-mechanical systems (RFMEMS) has led to the possibility of wide-range tunable filters with low current consumption, low distortion and potentially low cost.

RFMEMS have also been used to tune distributed filters. The centre-frequency of this class of filter can be altered by direct physical transmission-line length adjustment [2]. Bandwidth tuning is less common in planar filters due to the difficulties of adjusting the inter-resonator coupling.

This paper investigates a wide centre-frequency and bandwidth tuning range filter utilizing lumped-distributed, coupled transmission-line resonators. The coupled resonator structures employed are particularly suitable for use with RFMEMS contact and capacitive switches. They allow wide range tuning of both resonant frequency and coupling coefficient, limited only by the electrical size of transmission-lines and the placement density of the RFMEMS devices. Futhermore, the use of multiple distributed tuning elements results in a flexible structure where the resonator unloaded Q remains independent of the tuning mechanism [3]. In order to achieve this, a modified comb-line topology is adopted, consisting of pairs of grounded, quarter-wavelength, coupled resonators whose input and output terminals are at the same end. The structure becomes tunable by incorporating switchable coupling capacitors and switchable ground-connections along the length of the resonator lines (Fig. 1). The advantages of this topology are three-fold; firstly, only a

single grounding switch is in-circuit regardless of the selected length, therefore the impact of resistive switch losses on resonator Q remains constant. Secondly, it retains a constant overlap region and coupling factor regardless of the coupled line length. Finally, because the electro-magnetic (EM) coupling between the transmission-lines is in anti-phase to the lumped capacitive coupling, very low coupling coefficients can be obtained regardless of coupled-line spacing.

Using mathematical models developed in Section II the coupling coefficient and transmission characteristics of the structure can be analyzed. The lumped-distributed capacitive coupling introduces an additional attenuation pole and it is shown that the anti-phase relationship between the modes of coupling allows this pole to be placed either above or below the primary passband.

The tuning performance of the filter is presented visually and discussed in Section III. The theoretical filter performance and synthesis procedure are verified through the design and measured results of a 3rd order lumped-distributed coupled-line filter realized in co-planar waveguide in Section IV.
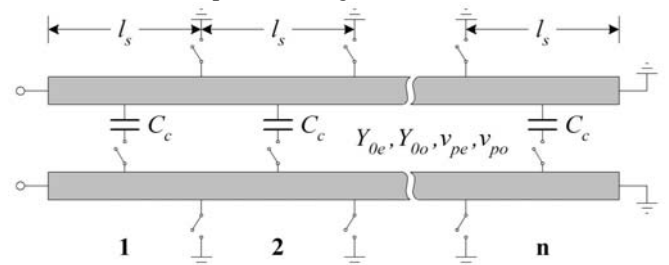

Fig. 1. Lumped-distributed, quarter-wave, coupled resonators. From [3].

II. LUMPED-DISTRIBUTED COUPLED LINES

A pair of lumped-distributed coupled-lines is shown in Fig. 1 having a per-unit-length coupling capacitance

$$C_{cm} = C_c / l_s \qquad (1)$$

and a coupled region length

$$l = n \cdot l_s . \qquad (2)$$

Fig. 1 shows the additional lumped capacitors and earth-shorts.

A. Admittance representation of the Circuit

An admittance representation of the lumped-distributed coupled-line section can be derived in several ways. A model which describes the true periodic nature of the lumped-distributed structure can be derived by using a combination of periodic and even- and odd-mode circuit analyses. However, it is also possible to model the circuit as purely distributed, leading to greatly simplified equations. A lumped-distributed

structure exhibits its first stopband when its guided wavelength approaches the periodic spacing of the lumped components. Well below this stopband, the structure can be accurately modeled as purely distributed. This approach is taken here.

A pair of coupled lines can be described in terms of their even- and odd-mode characteristic admittances (Y_{0e}, Y_{0o}) and phase velocities (v_{pe}, v_{po}). In the quasi-static case these even- and odd-mode parameters can be represented in terms of equivalent, lumped, per-unit-length inductances and capacitances as shown in Fig. 2 [4]. The relationships are

$$Y_{0e} = \sqrt{\frac{C_a}{L_a + L_m}} \,, \; Y_{0o} = \sqrt{\frac{C_a + 2C_m}{L_a - L_m}} \,, \quad (3)$$

$$v_{pe} = \sqrt{C_a(L_a + L_m)} \text{ and } v_{po} = \sqrt{(C_a + 2C_m)(L_a - L_m)} \quad (4)$$

where C_a and L_a are the self-capacitance and inductance of one of the lines and C_m and L_m are the mutual capacitance and inductance between the lines. Equations (3) and (4) can be rearranged to find the value of the equivalent lumped elements.

$$C_a = \frac{Y_{0e}}{v_{pe}}, \; C_m = \frac{1}{2}\left[\frac{Y_{0o}}{v_{po}} - \frac{Y_{0e}}{v_{pe}}\right], \quad (5)$$

$$L_a = \frac{1}{2}\left[\frac{Z_{0e}}{v_{pe}} + \frac{Z_{0o}}{v_{po}}\right] \text{ and } L_m = \frac{1}{2}\left[\frac{Z_{0e}}{v_{pe}} - \frac{Z_{0o}}{v_{po}}\right] \quad (6)$$
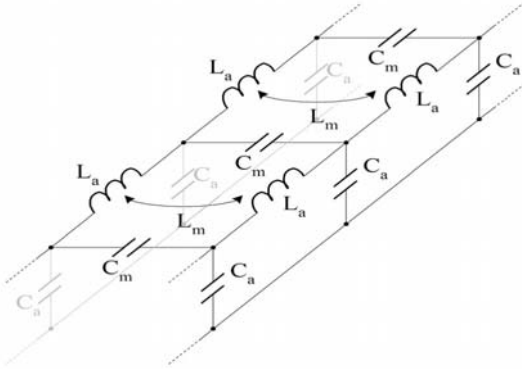

Fig. 2. Lumped equivalent circuit of coupled transmission lines

Additional inter-line coupling capacitance, C_{cm}, will have no effect on the parameters C_a, L_a and L_m and, as a consequence, the even mode parameters, Y_{0e} and v_{pe}, will remain unchanged. However, the odd-mode parameters will be affected and by making use of (3) to (6) the new values, Y'_{0o} and v'_{po}, can be expressed in terms of the original odd mode parameters and the additional, per-unit-length coupling capacitance, C_{cm}. The result is

$$v'_{po} = v_{po}\sqrt{\frac{Y_{0o}}{Y_{0o} - 2v_{po}C_{cm}}} \quad (7)$$

and

$$Y'_{0o} = \sqrt{Y_{0o}(Y_{0o} - 2v_{po}C_{cm})} \quad (8)$$

The admittance parameters of a symmetrical two port network are related to the even and odd-mode input admittances by the following two expressions.

$$y_{11} = \frac{y_{11e} + y_{11o}}{2} \quad \text{and} \quad y_{12} = \frac{y_{11e} - y_{11o}}{2} \quad (9)$$

Since the one-port even- and odd-mode input admittances of the lumped-distributed coupled-line model both have the form

$$y_{11e,o} = -jY_{0e,o}\cot\theta_{e,o} \quad (10)$$

where $\theta_{e,o}$ are the even or odd mode coupled-line phase lengths, the two port admittance parameters can be written as

$$y_{11} = -\frac{j}{2}\left(Y_{0e}\cot\left(\frac{\omega \cdot l}{v_{pe}}\right) + Y'_{0o}\cot\left(\frac{\omega \cdot l}{v'_{po}}\right)\right) \quad (11)$$

and

$$y_{12} = -\frac{j}{2}\left(Y_{0e}\cot\left(\frac{\omega \cdot l}{v_{pe}}\right) - Y'_{0o}\cot\left(\frac{\omega \cdot l}{v'_{po}}\right)\right). \quad (12)$$

where ω is the angular velocity and l is the coupled line length.

B. Coupling Coefficient Analysis

Using the formulation developed in [5] the coupling coefficient of the lumped-distributed coupled-line structure can be found from its simulated frequency response. Typical results are shown in Fig. 3 where the coupling coefficient for a pair of coupled microstrip lines is plotted against the total lumped capacitance for various values of coupled line spacing, *s*. The change in gradient of the coupling coefficient, from negative to positive, is indicative that, for this coupled-line configuration, the distributed electro-magnetic (EM) coupling is primarily magnetic in nature and is in anti-phase to the direct capacitive coupling. The result is that, at low values of lumped coupling capacitance, the coupling coefficient is actually reduced allowing the coupling coefficient, and therefore the filter bandwidth, to be controlled down to a very low value without the need for large coupled-line spacings.
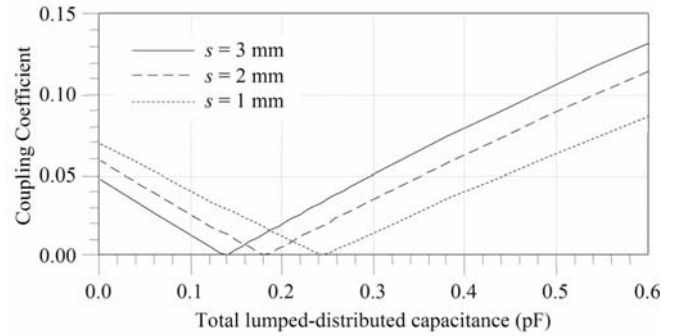

Fig. 3. Coupling coefficient of lumped-distributed coupled lines indicating that the capacitive coupling (due to C_m+C_{cm}) is in anti-phase to the EM coupling (dominated by L_m).

The electric and magnetic coupling coefficients are the ratio of coupled to stored electric and magnetic energy. In the quasi-static case they can be derived from the capacitance and inductance elements of the lumped equivalent circuit. Summing the two yields the total mixed coupling which, for this configuration takes the form

$$k = \left|\frac{C_m + C_{cm}}{C_a + C_m + C_{cm}} - \frac{L_m}{L_a}\right|. \quad (13)$$

C. Transmission Characteristics

Using two-port circuit analysis the ratio of input to output voltage or voltage attenuation function, $A(j\omega)$, for a pair of

same-end-shorted coupled lines terminated in a source and load admittance, Y_g, can be found from (11) and (12) as

$$A(j\omega) = \frac{(jY_{0o}\cot\theta_o - Y_g)(Y_g - jY_{0e}\cot\theta_e)}{j2Y_g(Y_{0e}\cot\theta_e - Y_{0o}\cot\theta_o)} \quad (14)$$

Poles of attenuation occur when the denominator of (14) is equal to zero. This condition is satisfied when $Y_{0o}\cot\theta_o = Y_{0e}\cot\theta_e$. For purely distributed, same-end-grounded, coupled lines in a non-homogenous medium the condition for a pole of attenuation is met only at dc. Complete transmission corresponds to zeros in the numerator which occur when either $jY_{0o}\cot\theta_o$ or $jY_{0e}\cot\theta_e$ equal Y_g. This indicates that the primary passband is centered between the even and odd mode quarter-wavelength frequencies, its width being dependent on the ratio of $|Y_g|$ to Y_{0e} and Y_{0o}. Further passbands occur at all odd harmonic frequencies.

The lumped capacitance C_{cm}, introduces an additional attenuation pole. At low values of capacitance, where the coupling is still primarily magnetic, the pole appears above the primary passband. As the capacitance is increased the pole frequency reduces until the pole and zero frequencies coincide and the primary passband disappears. The value of capacitance at which this occurs can be found by substituting (5) and (6) into (13) and setting $k = 0$. This value corresponds to the point of gradient change in Fig. 3 and is given by

$$C_{cm0} = \frac{Y_{0e}\left(v_{po}^2 - v_{pe}^2\right)}{2v_{po}v_{pe}^2}. \quad (15)$$

When the lumped capacitance is larger than this value the pole appears below the primary passband. Accordingly, two regions of variable coupling coefficient can be defined; above and below C_{cm0}. Using adjustable lumped capacitance in the lower region results in a bandwidth-tunable filter with better high-side rejection. However, the maximum achievable bandwidth in this case occurs when the lumped capacitance is set to zero and will be dictated by the EM coupling that can be achieved. The maximum amount of EM coupling that can be obtained from a pair of same-end-grounded coupled lines is limited by the degree to which the structure supports unequal odd- and even-mode wave velocities. In practice this will limit the use of the high-side pole variant to narrow-band filters.

However, using adjustable coupling capacitance in the second region (above C_{cm0}), although giving compromised upper stopband performance, does lead to a design where the maximum bandwidth is limited only by the capacitance value.

III. FILTER REALIZATION AND TUNING

In order to synthesize the filter, the design equivalence equations defining the characteristics of the resonant sections and the admittance inverters were generated by the generic model comparison method described in [6]. This method compares the admittance and phase of sections of the filter to be designed with those of a generic, inverter-coupled filter, forcing the two to correspond at specific points in the filter passband. The development of this method for this application is described in [7]. Using the equations developed by this method a filter can be designed from a number of lumped-distributed coupled-line sections. Solving these equations results in specific values of coupling capacitance and line length for a given filter centre frequency and bandwidth.

Once these initial design values have been selected the filter is tuned by the discrete switching of ground connections and coupling capacitors. Since the tuning is not continuous only certain values of centre frequency and bandwidth can be obtained. Furthermore, the relationships between coupling capacitance, resonator length, fractional bandwidth and centre frequency are not linear.

From (3) and (4) it is clear that the coupling capacitance acts to reactively load the transmission lines, altering their odd-mode characteristic impedance and phase velocity. As the coupling capacitance is tuned, the effective phase velocity and consequently, the resonant frequency of the coupled lines alters. However, this change in phase velocity is not consistent throughout the filter. To achieve the impedance transformation required in practical transmission-line filters the coupling capacitors of the filter end sections must be significantly larger than those of the interior sections. Changing the bandwidth involves scaling the inter-resonator coupling throughout the filter and the disproportionate size of the end section coupling capacitors means that their scaling has a greater effect on the phase velocity. This leads to misalignment of end and interior section resonant frequencies, distorting the filter shape. Continuously variable resonator lengths could compensate for this by incremental adjustment however this is not possible in the discrete design. The result is that a good filter shape is only available at certain tuning points.

In order to gain an appreciation of this effect it is helpful to plot the points where good filter shape can be achieved on the two-dimensional tuning surface of the lumped-distributed coupled resonator filter; fractional bandwidth versus centre frequency. To do so, a measure of a particular tuning point's deviation from the desired filter characteristics is required. One way of expressing this deviation is to determine the line length and coupling capacitance of each filter section required for a particular fractional bandwidth and centre frequency. The deviations of each of these length and capacitance values from the available discrete values can then be combined to give an overall error value. Plotting this error value on a contour plot versus centre-frequency and bandwidth gives a visual representation of the tuning performance of a particular filter. As an example the error contour plot for the experimental filter to be introduced in Section IV is shown in Fig. 4. The experimental filter has four lumped-distributed coupled-line sections and eight length (l_s) and capacitance (C_c) parameters. Due to the filter symmetry only 4 of these are needed to find the overall error. This error value will vary between zero, for a perfect filter shape, and two, for maximum error. In the latter case every length and capacitance parameter is exactly midway between discrete tuning points.
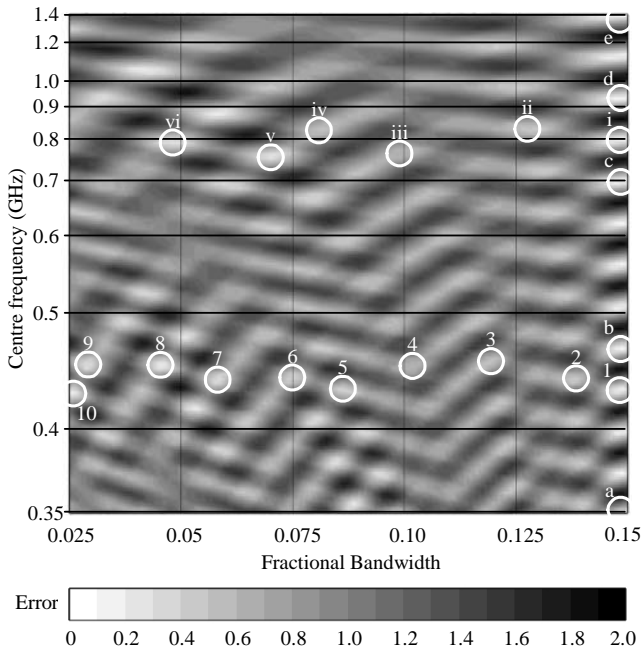
Fig. 4. Contour plot of filter shape error on the two-dimensional tuning space; fractional bandwidth and centre frequency. The series of data points on the plot are discussed in Section IV, each of these series are generated from a compound reconfiguration of line length and lumped coupling capacitance.

The plot shows a series of good tuning points at the initial design fractional bandwidth (which in this case is equal to 0.15), uniformly spaced at frequencies corresponding to the discrete length tuning points. This occurs because, in this design, all of the filter sections have the same number of tunable length segments resulting in the synchronous tuning of their electrical lengths.

For different values of fractional bandwidth the relationship becomes more complex. This is due to the changes in per-unit-length coupling capacitance. The result is that the points on the tuning surface which yield good filter performance follow non-equi-spaced lines diverging as the centre frequency increases.

IV. EXPERIMENTAL RESULTS

To verify the theoretical analysis and to test the lumped-distributed coupled-line filter's tuning capabilities a third order filter with 16 tunable segments was fabricated based on a Butterworth prototype and a micro-strip transmission line realization. The resultant filter is layout is shown in Fig. 5. The filter measures approximately 44 x 240mm.
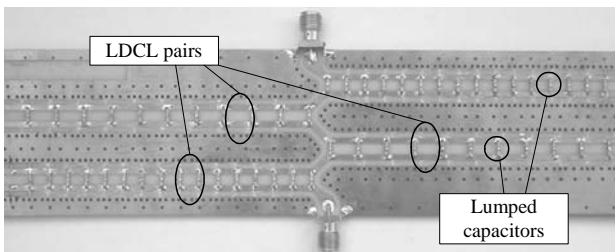

Fig. 5 Partially cropped image of 3-element filter with four pairs of LDCLs.

A model for the lumped-distributed coupled-line filter was built up from analytical and full-wave EM simulations using Agilent Technologies ADS. This model was used to simulate the response of the experimental filter. This is presented in Fig. 6 along with the measured results of the filter at the initial design frequency and bandwidth. For medium bandwidths and low filter order the upper stopband rejection is poor, however, the simulated response shows reasonable correlation with the measured results. The increase in frequency of the low-side attenuation pole has been shown to be caused by cross-coupling between non-adjacent resonators.
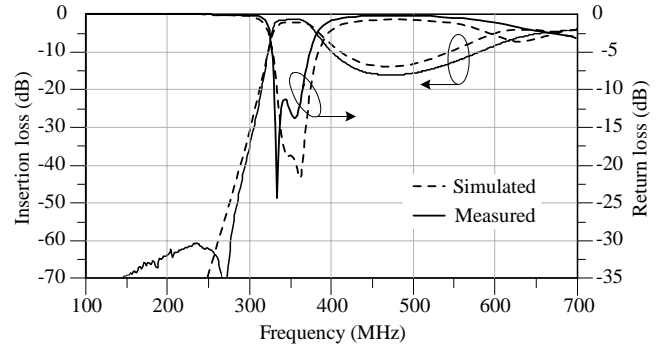

Fig. 6. Measured (solid) and simulated (broken line) response for lumped-distributed coupled line filter at the initial design frequency and bandwidth.

A. Centre-Frequency Tuning

Although many different centre-frequency tuning states are possible, the largest number having constant fractional bandwidth occur at the design value of 0.15 as discussed in Section III. These tuning states can be obtained by switching all the coupling capacitors in circuit and discretely varying the length of all the coupled line sections synchronously. A selection (indexed a to e in Fig. 4) of the 16 possible tuning states are shown in Fig. 7 along with the corresponding simulated responses. The filter gives almost constant fractional bandwidth across the complete tuning range except for a slight reduction at low values of coupled-line length (from 14% to 11.5%). The variation in insertion loss across the tuning range is also minimal. This reflects a constant unloaded Q of the resonators regardless of tuning position.
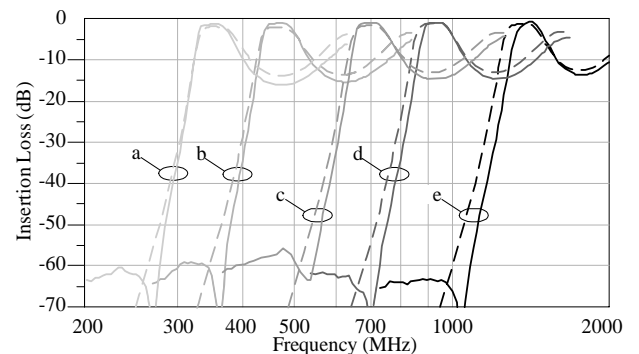

Fig. 7. Simulated (broken line) and measured (solid line) results for five of the 16 possible tuning states of the experimental lumped-distributed coupled-line filter. The indexing terms, a to e refer to Fig. 4. Data from [3].

B. Bandwidth Tuning

To test the bandwidth tuning capabilities of the filter two groups of sample points were chosen which had similar centre-frequencies but a range of bandwidth values. The two groups are shown in Fig. 4 around 800MHz and 450MHz. Each of the points corresponds to a local minimum in the error function.

Each of these points was measured using the experimental filter and the results of the different tuning states are shown in Fig. 8 through Fig. 10. For clarity, the measured results for the 430MHz cluster have been grouped around common centre-frequencies and split over two plots. The variation in centre frequency is a function of the density of configurable elements.
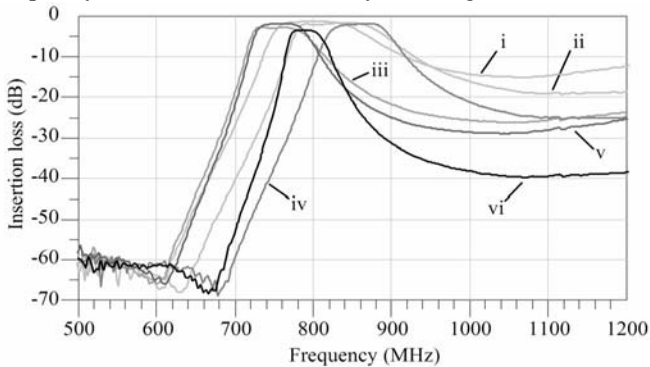

Fig. 8. Measured insertion loss of experimental lumped-distributed coupled-line filter for 6 bandwidth tuning points circa fc=800MHz.
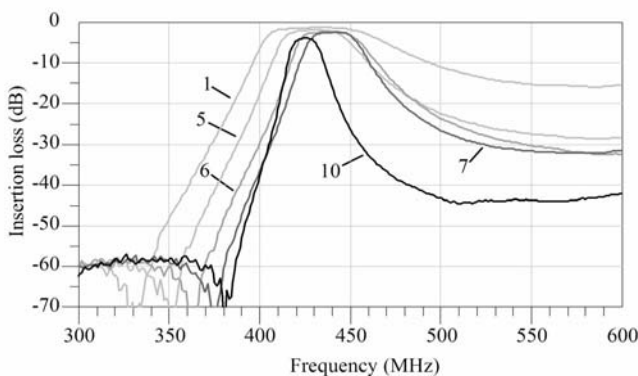

Fig. 9. Measured insertion loss of experimental lumped-distributed coupled-line filter for 5 of the 10 bandwidth tuning points circa fc=450MHz.

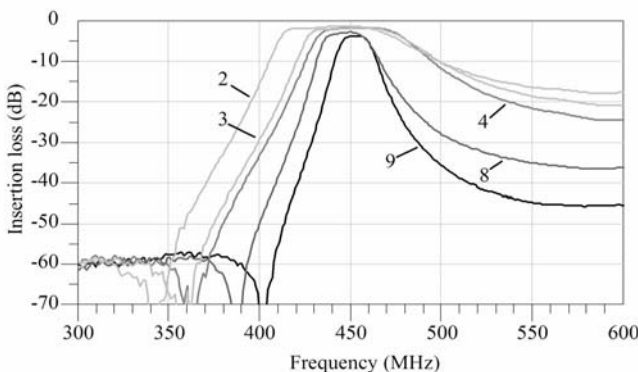

Fig. 10. Measured insertion loss of experimental lumped-distributed coupled-line filter for 5 of the 10 bandwidth tuning points circa fc=450MHz.

C. Discussion

The results shown here demonstrate that both wide range centre-frequency and bandwidth tuning are possible using the lumped-distributed coupled-line topology. The experimental filter could be tuned in discrete steps over two octaves of centre-frequency, 350 MHz – 1.4 GHz, with little degradation in the response. In addition, a number of different bandwidth settings could be selected, ranging from 3.8% to 14.5%; a 3.8:1 tuning range. A disadvantage is that the tuning ranges are not uniform; at lower frequencies there is a greater choice of both centre-frequency and bandwidth. However, it may be possible to provide more consistent tuning resolution through the use of reconfigurable resonators which can be switched either in parallel or series [8].

V. CONCLUSION

The lumped-distributed, coupled-line filter topology described in this paper was developed to provide a filter structure which could be tuned in both bandwidth and centre-frequency over a wide range. The shunt and parallel connections of the multiple distributed switching elements means that the losses remain constant regardless of the number of switching elements employed. The number and range of the tuning steps is thus only limited by the number of switching elements, not by losses in the filter structure itself. The anti-phase relationship between the electro-magnetic and capacitive coupling coefficients of lumped-distributed coupled-lines allows for very low fractional bandwidths without the need for widely spaced lines. The performance of the lumped-distributed coupled-line filter has been verified through experimental results.

REFERENCES

[1] J.R. Macleod, M.A. Beach, P.A. Warr, and T. Nesimoglu, "A Software Defined Radio Receiver Test-bed," in *Proc. 54th Veh. Technol. Conf.*, VTC 2001 Fall, IEEE VTS 54th , Vol. 3, 2001, pp. 1565-1569.
[2] J.R. Macleod, T. Nesimoglu, M.A. Beach, P.A. Warr, "Miniature distributed filters for software re-configurable radio applications," in *Proc. IST Mobile Wireless Telecommun. Summit 2002*, June 2002, pp. 159-163.
[3] B. Carey-Smith, P. A. Warr, M. A. Beach, T. Nesimoglu, "Tunable lumped-distributed capacitively-coupled transmission-line filter," *IEE Electron. Lett.,* Vol. 40, pp. 434 – 436, Apr 2004.
[4] R. Mongia, I. J. Bahl, P. Bhartia, *RF and microwave coupled-line circuits*. Norwood, MA: Artech House, 1999, pp 150 – 151.
[5] J-S. Hong, M. J. Lancaster, "Couplings of microstrip square open-loop resonators for cross-coupled planar microwave filters," *IEEE Trans. Microwave Theory Tech.*, vol. MTT-44, pp. 2099 -2109, Nov. 1996.
[6] G. L. Matthaei, L. Young, E. M. Jones, *Microwave filters, impedance-matching networks and coupling structures*. Norwood, MA: Artech House, 1980, pp 636 – 638.
[7] Bruce E. Carey-Smith, Paul A. Warr, Mark A. Beach, and T Nesimoglu, 'Wideband Tunable Planar Filters using Lumped-Distributed Coupled Transmission Lines', *IEEE Transactions on Microwave Theory and Techniques*, Accepted for Publication, expected in Feb 05.
[8] B. Carey-Smith, P. A. Warr, M. A. Beach, T. Nesimoglu, "A MEMS-ready wide tuning range planar resonator with application to microwave flexible filters," in Proc. Asia-Pacific Microwave Conf., APMC 2003, Nov. 2003, pp 1581 – 1584.